

Cryogenic High-Resolution X-Ray Spectrometer Development

Stephan Friedrich



Lawrence Livermore National Lab

Owen Drury, Thomas Niedermayr

Simon Labov



Lawrence Berkeley National Lab

Tobias Funk

Steve Cramer

Funding: DOE-OBER, NIH-GM, NSF-IMR, NASA SR&T

ESRF, February 14th, 2003

Cryogenic Detector Development at LLNL

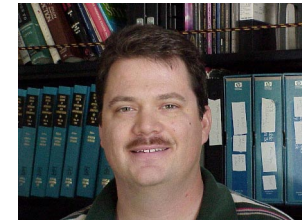
Advanced Detector Group
Bill Craig, Group Leader

Cryogenic Detector Group
Stephan Friedrich

Radiation Detection Center
Simon Labov, Director

Microcalorimeters (TES)

Tunnel Junctions (STJ)



X-ray Detectors

(S. Terracol)

X-ray Astronomy

(NASA)

Atomic (ion) physics

Prof. Briand, U Paris

Gamma Detectors

(T. Miyazaki)

Nucl. Non-proliferation

(DOE NA-22)

Prof. Freeman, UCD

Dr. Vogt, IAEA

Neutron Detectors

(T. Niedermayr, D. Hau)

Nuclear Physics

(DOE NA-22)

Prof. Vujic, UC Berkeley

Astrophysics

Dr. Wang, LLNL

X-ray Detectors

(S. Friedrich, O. Drury)

Biophysics

(NIH-GM, DOE-OBER)

Prof. Cramer, UC Davis

Material Science

(NSF-MRI)

Prof. Opila, U Delaware

Prof. Harris, Stanford

Outline: Why Cryogenic Detectors?

- Why low T?
 - Low thermal noise
 - Small excitation energies
- High energy resolution

- Which technologies?

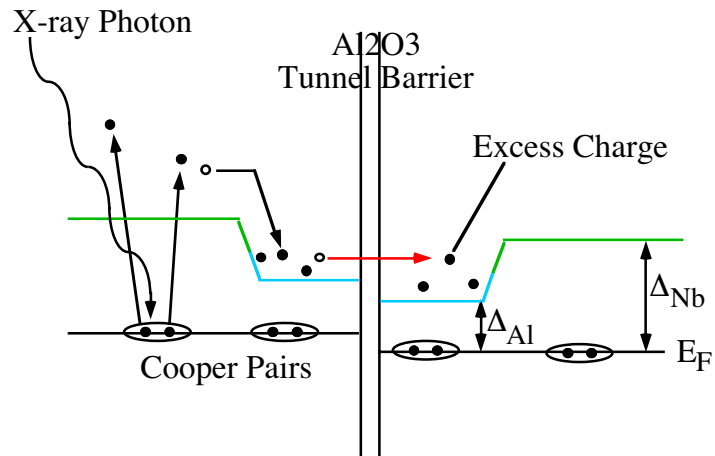
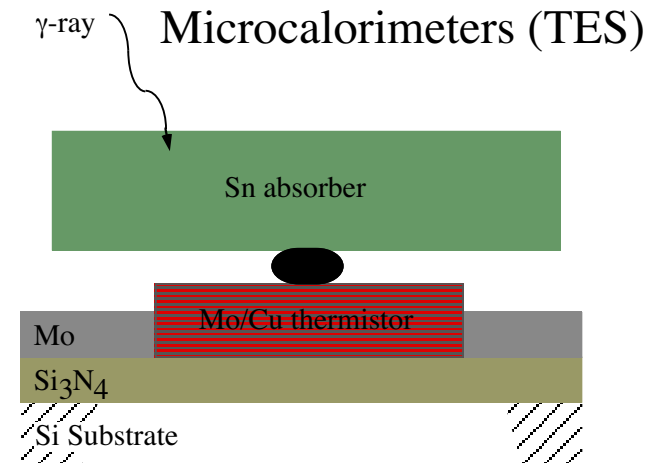
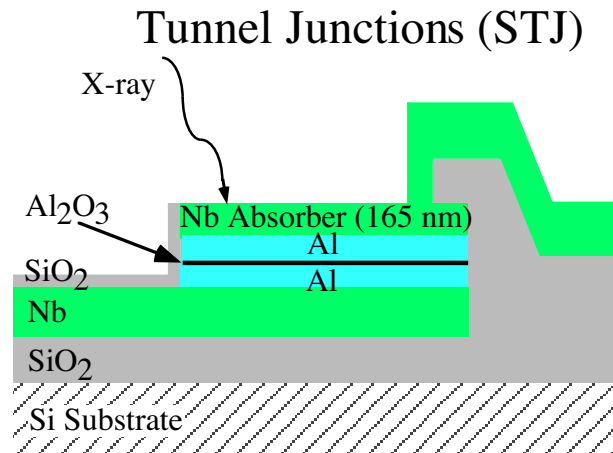
	Tunnel Junctions	Microcalorimeters
Operating Principle	$E \rightarrow \Delta Q$	$E \rightarrow \Delta T$
Resolution (0.1 to 6 keV)	2 - 12 eV FWHM	2 - 5 eV FWHM
Max. count rate	~10,000 cts/s	~500 cts/s

Both detectors have small pixel sizes ($\sim 0.2 \text{ mm}$)² and are operated around 0.1 K.

- What for?

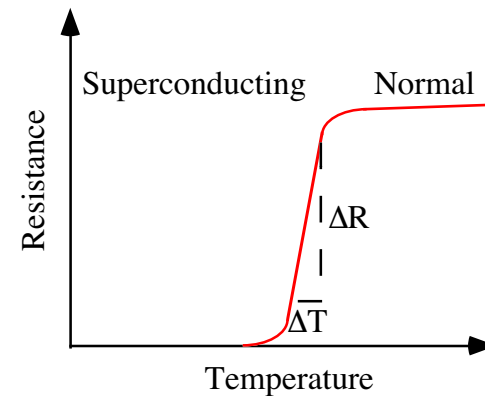
Fluorescence-detected absorption spectroscopy of dilute samples

Superconducting Detector Technologies



Signal = Current Pulse

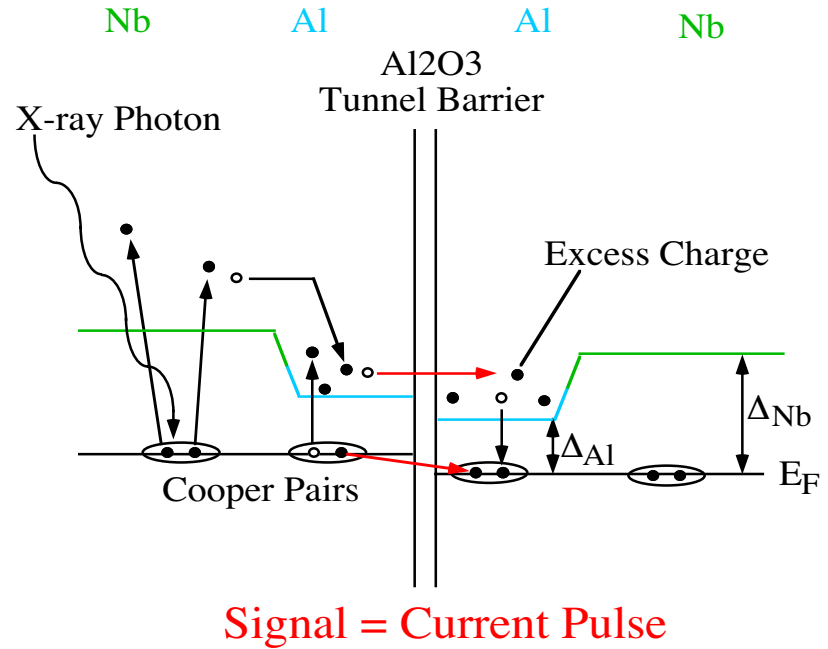
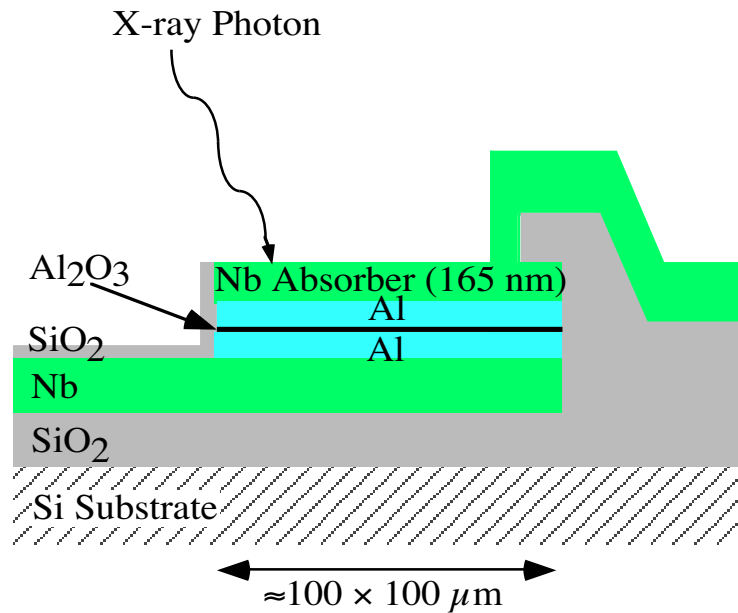
High resolution, faster



Signal = Resistance Change

Highest resolution, slower

Superconducting Tunnel Junction Detectors

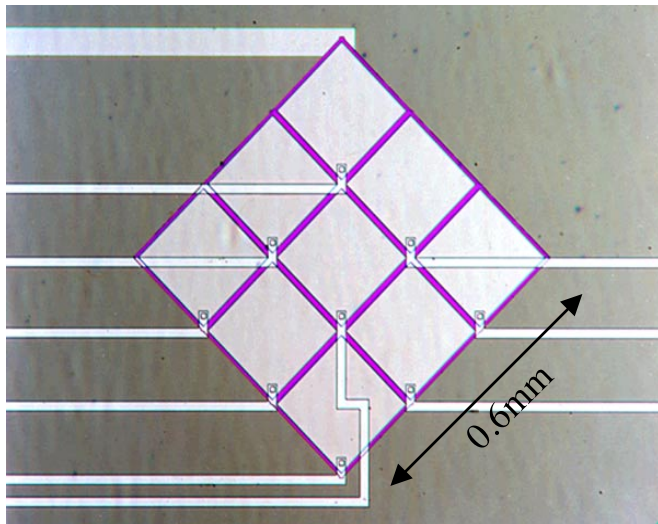


$$\Delta E_{\text{FWHM}} = 2.355\sqrt{(\epsilon E(F+1+1/\langle n \rangle))}$$

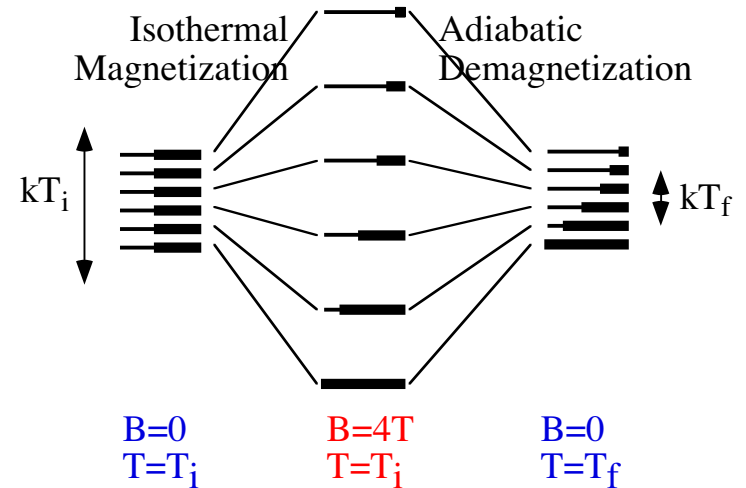
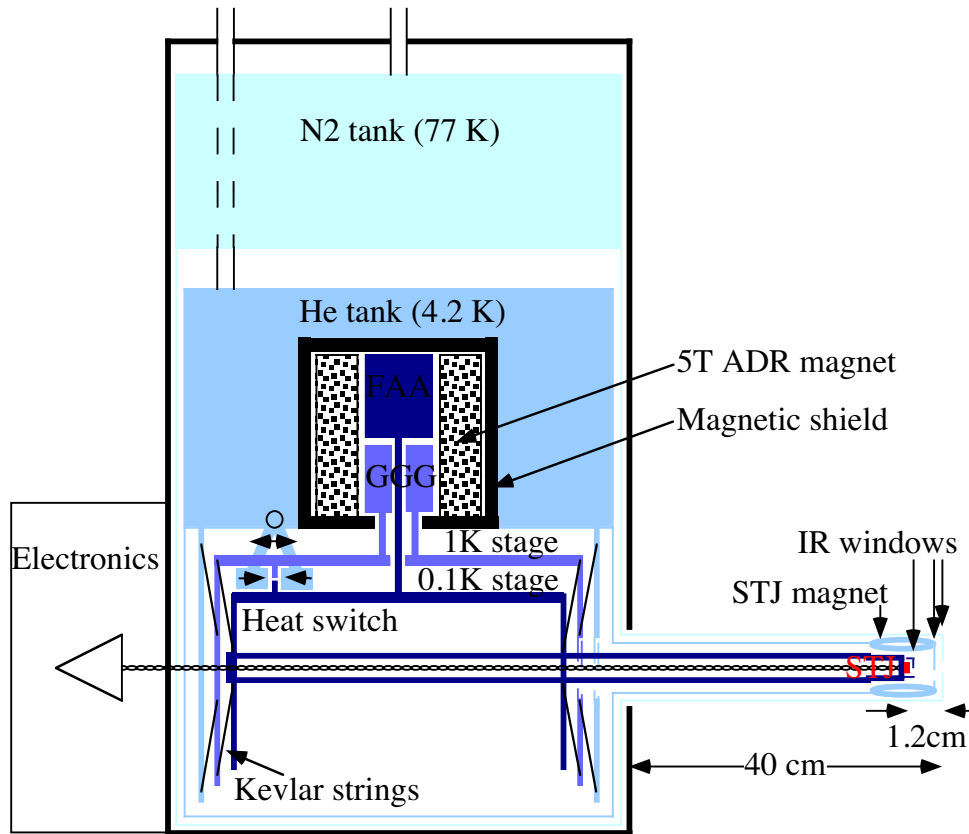
Small energy gap ($\Delta \approx 1 \text{ meV}$) \Rightarrow High energy resolution ($\approx 10 \text{ eV FWHM}$)
 Short excess charge life time (μs) \Rightarrow (Comparably) high count rate ($\approx 10,000 \text{ counts/s}$)

Two-Stage ADR with Cold Finger

- 70 mK base T, 20h below 0.4K
- 3×3 array at $\approx 15\text{mm}$ $\Rightarrow \Omega/4\pi \approx 10^{-4}$
- $\approx 15\text{eV}$ FWHM, $>100,000$ cts/s max

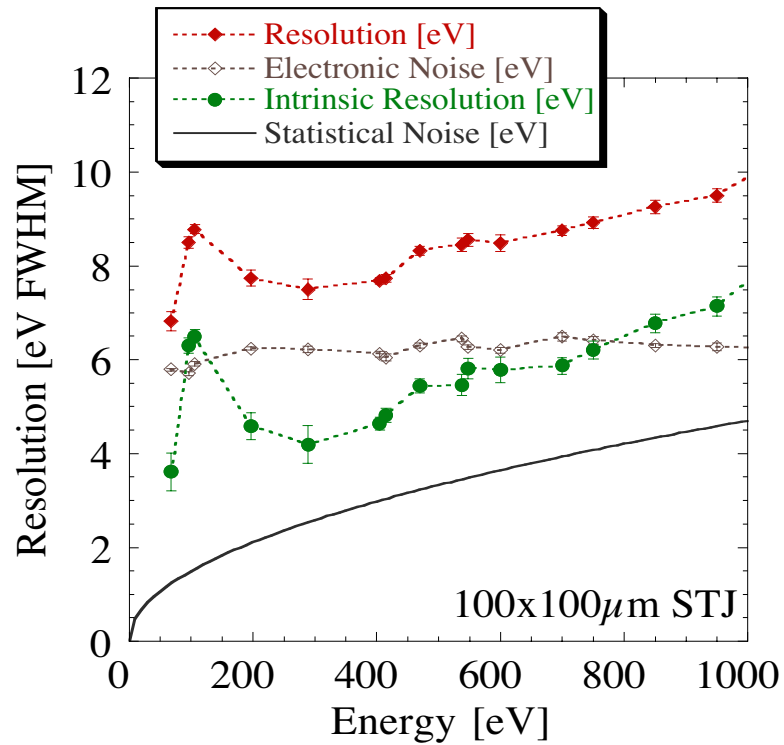


Adiabatic Demagnetization Refrigeration

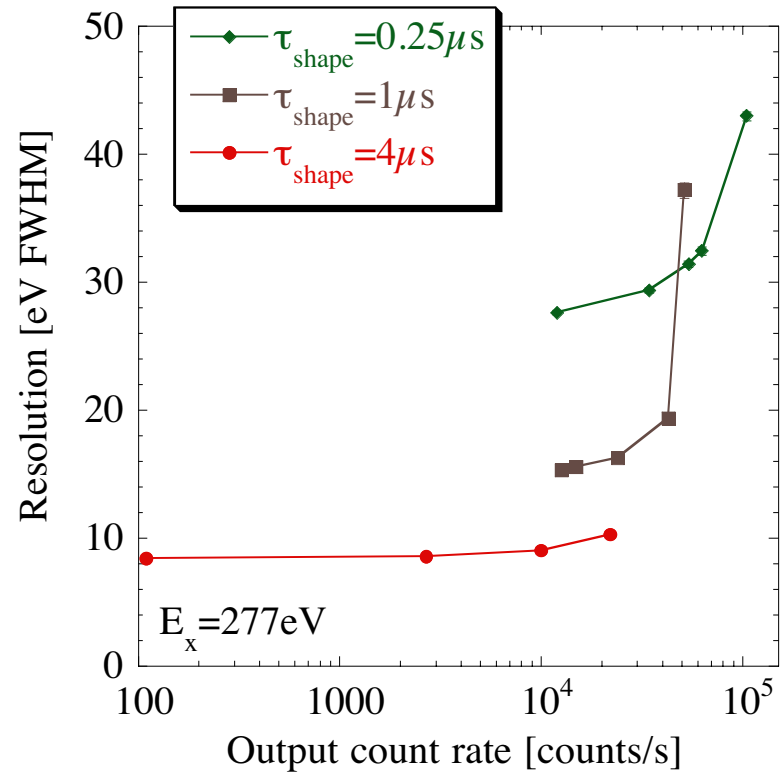


- 1) Close heat switch
- 2) Apply B (lower entropy S)
- 3) Open heat switch (decouple T)
- 4) Reduce B slowly (keeping entropy constant \Rightarrow reduce T)

STJ Detector Performance

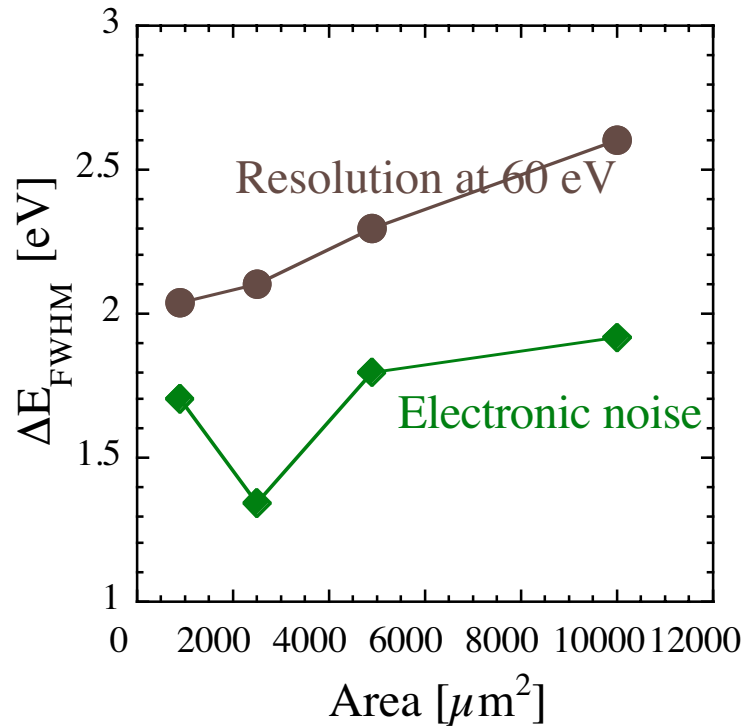


≤ 10 eV resolution below 1keV

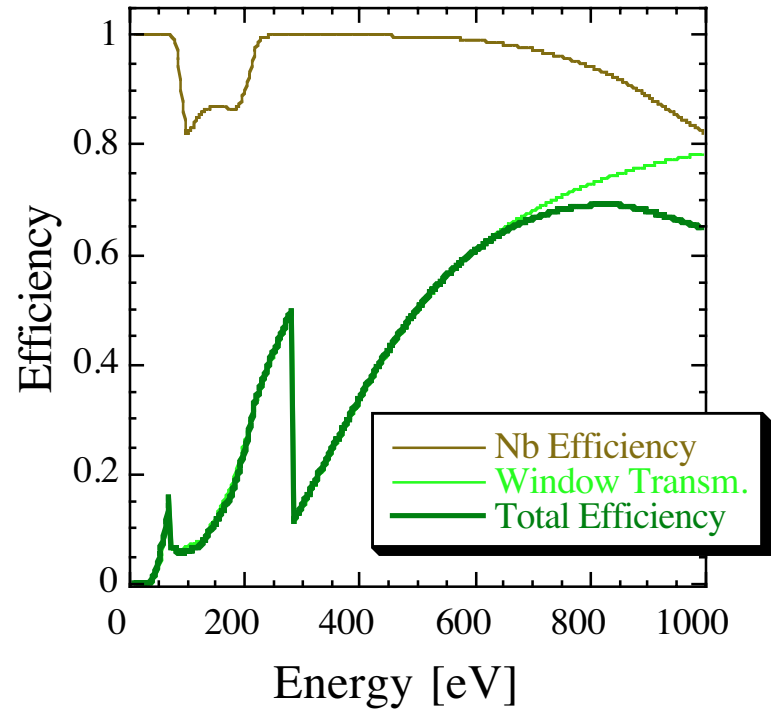


$\geq 10,000$ counts/s throughput

STJ Detector Performance



Trade-off between area and resolution



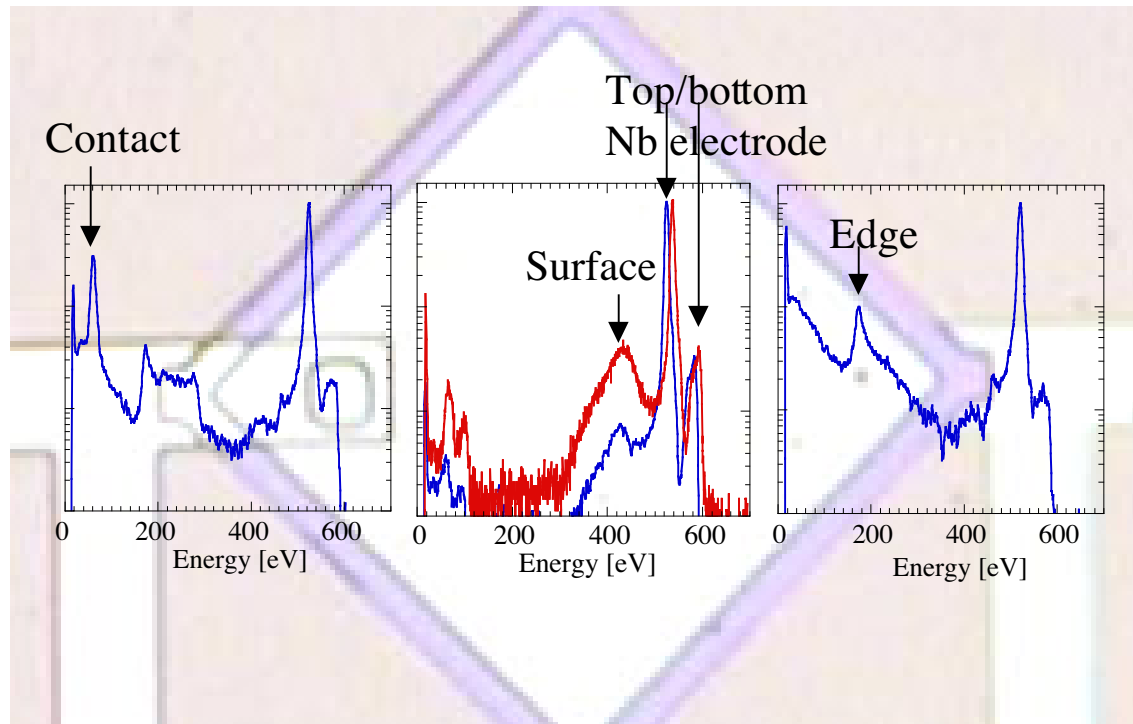
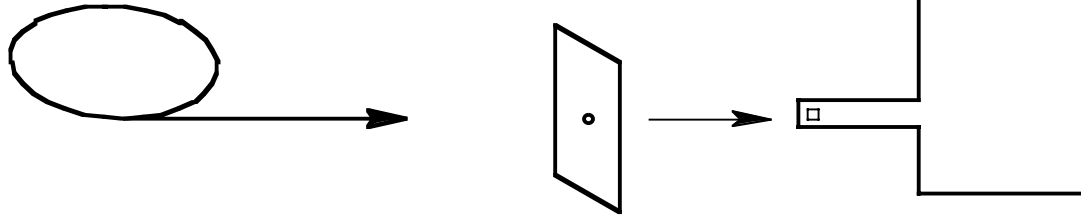
Trade-off between efficiency and resolution

Lineshapes

Synchrotron beam
 $50 \text{ eV} \leq E_x \leq 2 \text{ keV}$

Aperture
movable in x and y

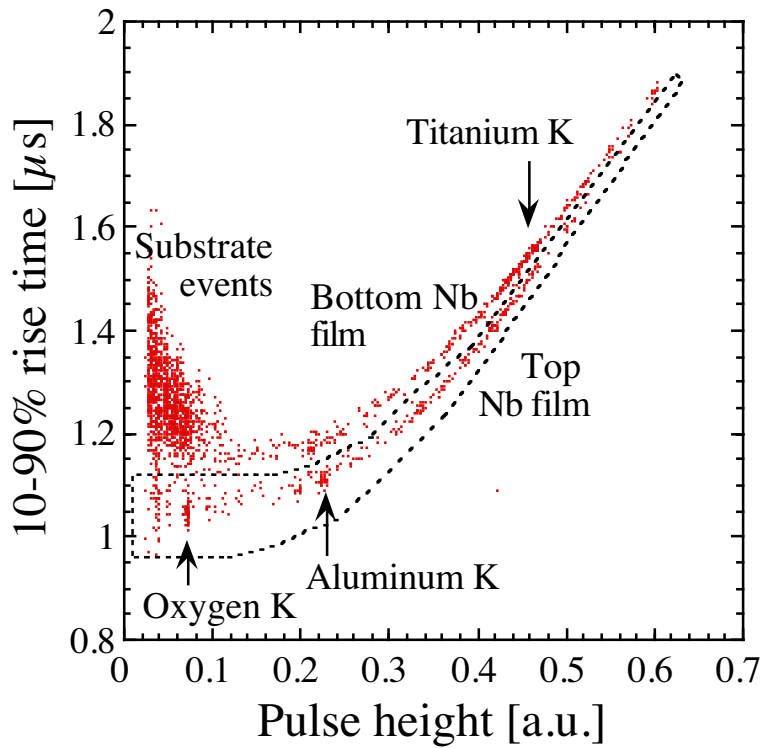
STJ Detector
on ADR snout



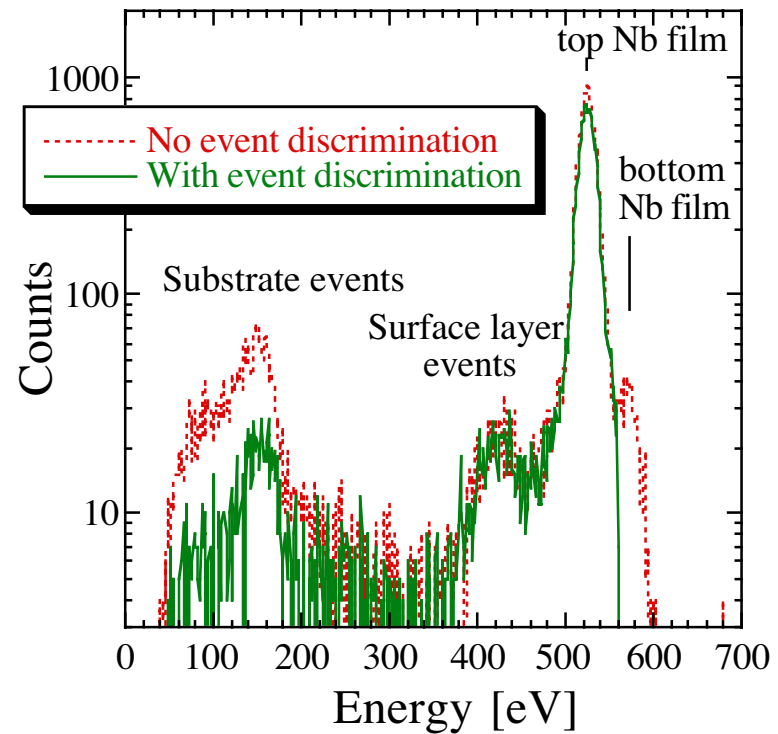
Artifacts can be greatly suppressed with apertures.

\Rightarrow Peak/Backgnd ≈ 1000

Digital Signal Processing



Rise time differences between top and bottom electrode and substrate

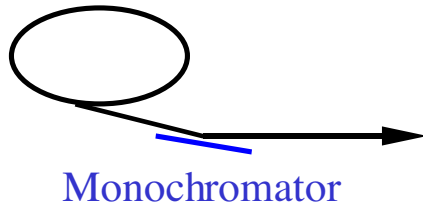


On-line event discrimination at 5000 cts/s to reduce artifacts

X-ray Absorption Spectroscopy

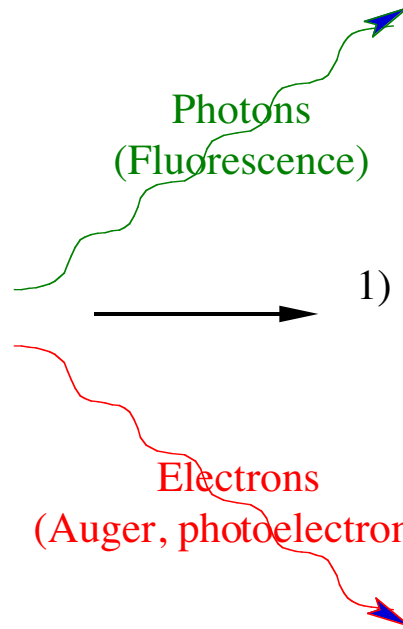
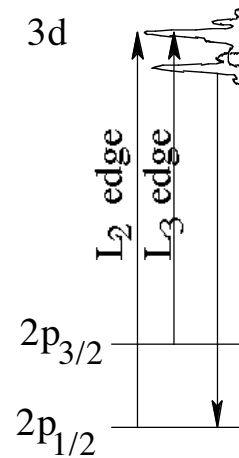
Synchrotron beam

Intense, monochromatic, tunable
 $I_0 \approx 10^{12}$ photons/s
 $\Delta E = 0.1 \text{ eV}$



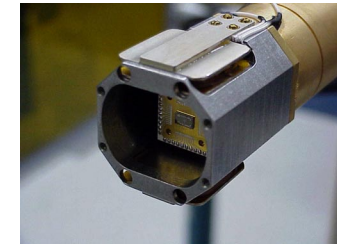
Sample x

Absorption $\mu_x(E)$



Detection

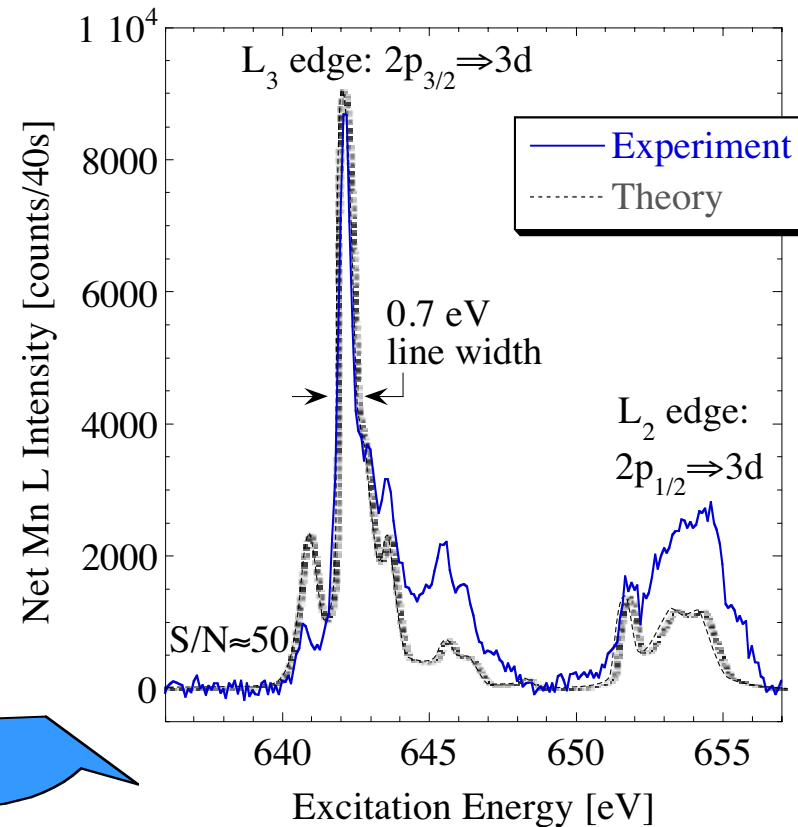
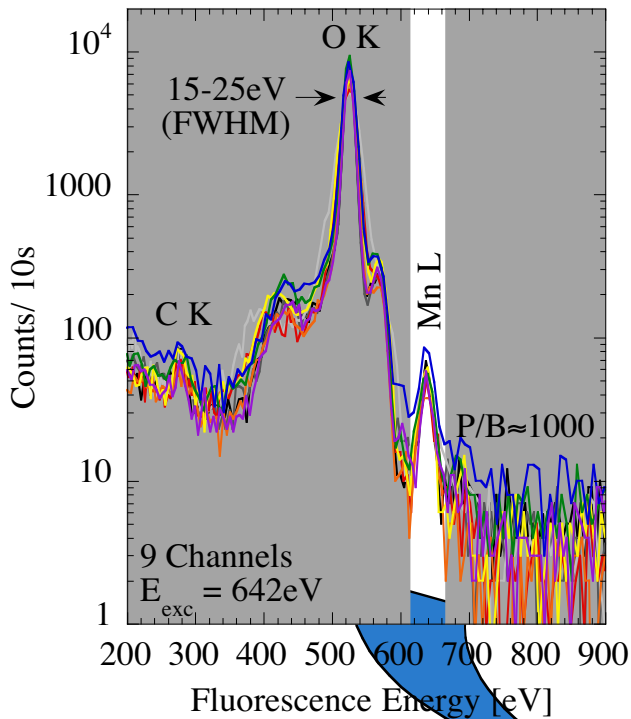
3) Fluorescence $\propto I_0 \cdot \mu_x(E)$



1) Transmission $\propto I_0 (1 - \mu_x - \mu_{\text{bgnd}})$
Thin samples
High background

2) Electron signal $\propto I_0 \cdot \mu_x(E)$
Surface sensitive
Moderate background

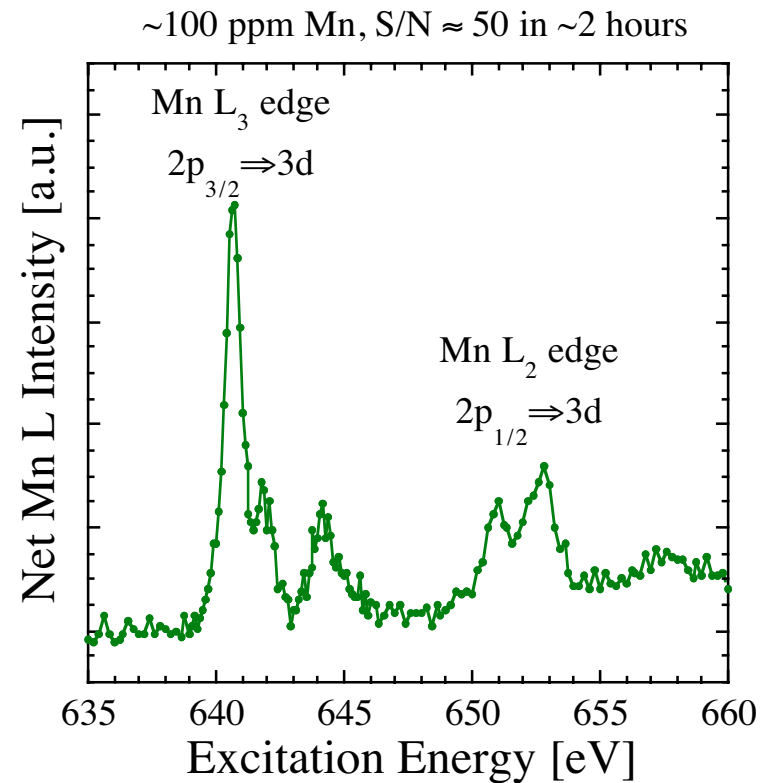
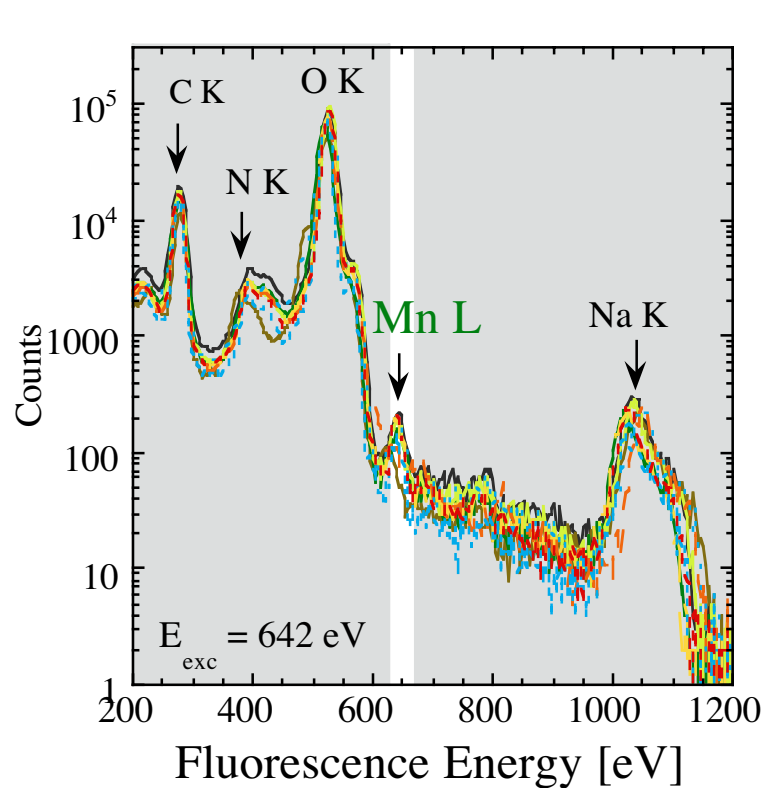
Absorption Spectroscopy on 840ppm Mn in MgO



Mn L fluorescence intensity \propto
Absorption by Mn \propto
Mn 3d vacancies

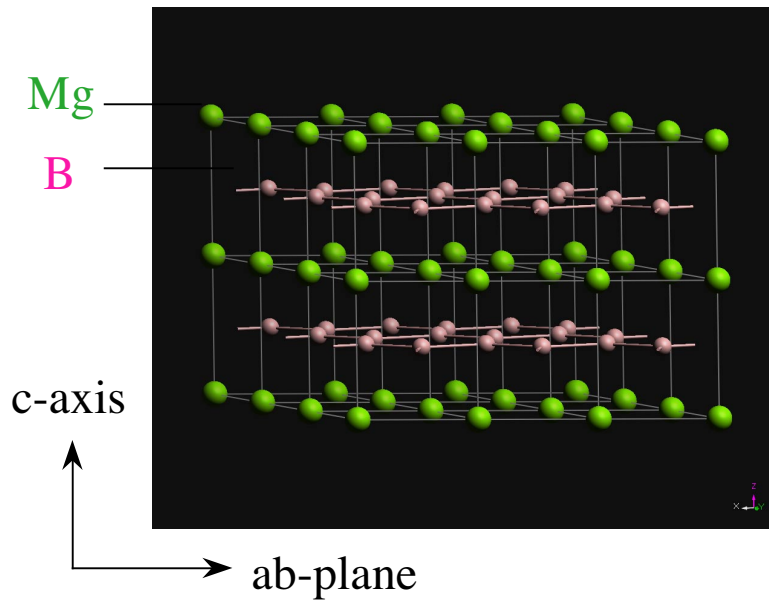
Multiplet Simulations:
Fine structure indicative of Mn^{2+}
in cubic crystal field $10Dq \approx 1.4eV$

X-Ray Absorption Spectroscopy on Proteins

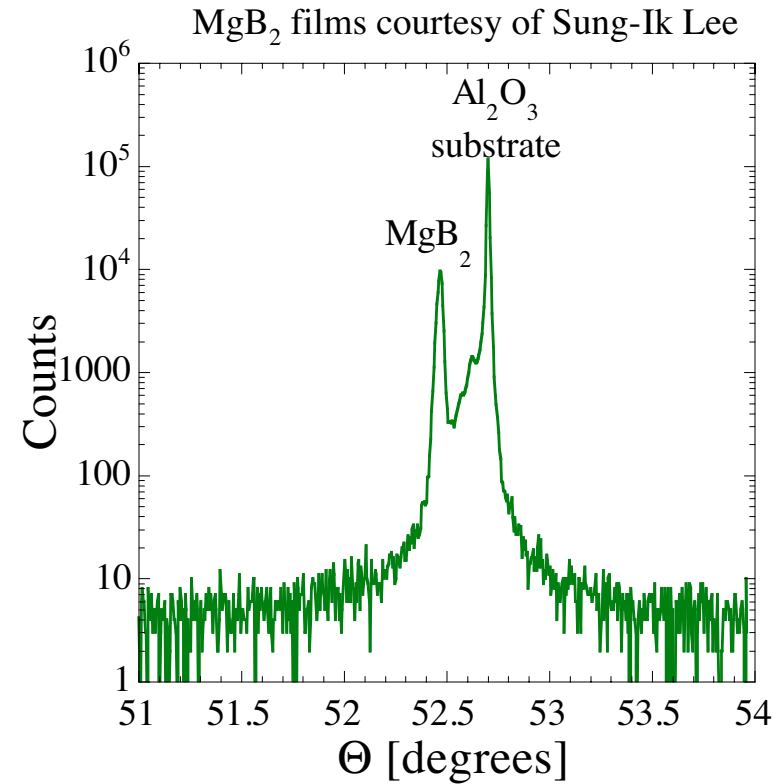


Spectrometer sensitivity is sufficient for ~100 ppm samples

MgB₂: Is the superconductivity anisotropic?

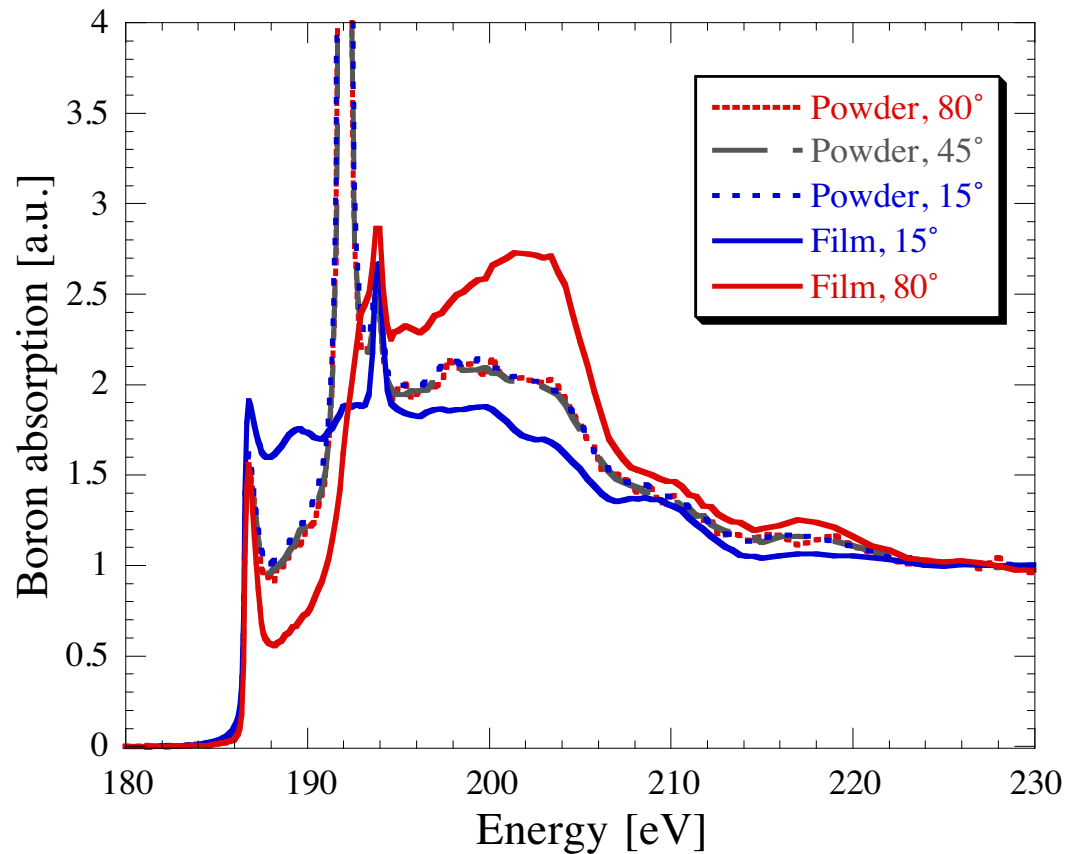


Mg donates ~ 2 electrons to the B sheets $\Rightarrow 2p^3$ configuration
Hybridized sp_2 levels are half-filled \Rightarrow Fermi level



	Bulk	Thin Film
Al ₂ O ₃	3.481 Å	3.481 Å
MgB ₂	3.522 Å	3.496 Å

Angle dependence: MgB₂ film vs powder

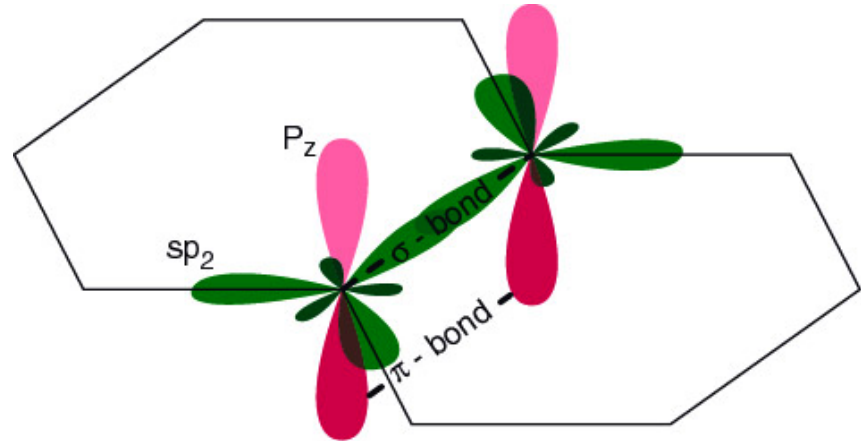
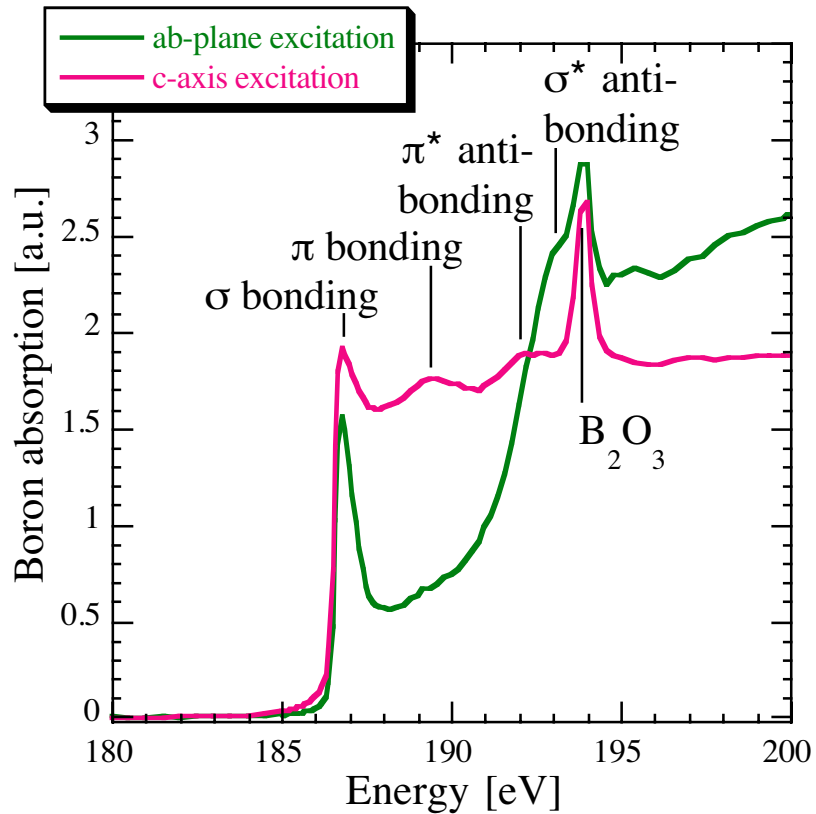


The angle of the horizontally polarized incident beam is measured relative to the sample surface, i.e. 80° means in-plane excitation.

The peak at 192 eV is due to an excitonic resonance. The peak at 194 eV is due to B₂O₃ at the surface.

The epitaxial MgB₂ film does show anisotropic absorption.
The powdered MgB₂ sample does not, as expected.

In-plane vs. out-of-plane excitation



ab-plane: $p_x, p_y \Rightarrow sp_2$ hybridized
 σ bonds, hexagonal

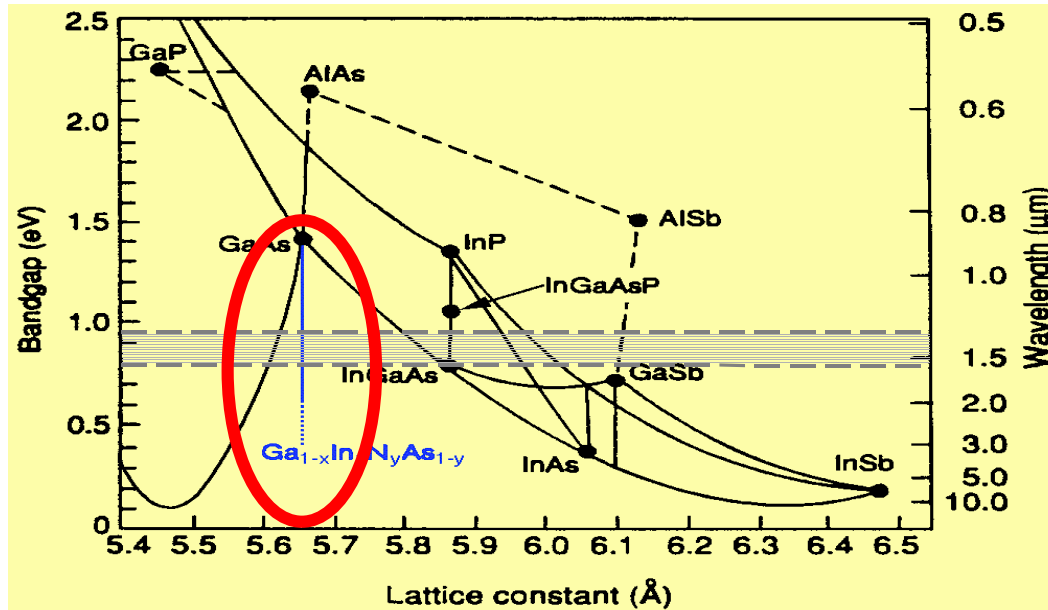
c-axis: $p_z \Rightarrow \pi$ bonds

The anisotropic electronic structure in MgB_2 is due to sp_2 -hybridization. Electronic density of states at E_{Fermi} is comparable in ab-plane and along c-axis.

GaInNAs: A material for 1.3-1.55 μ m lasers



Collaboration with V. Lordi from Prof. Harris' group at Stanford



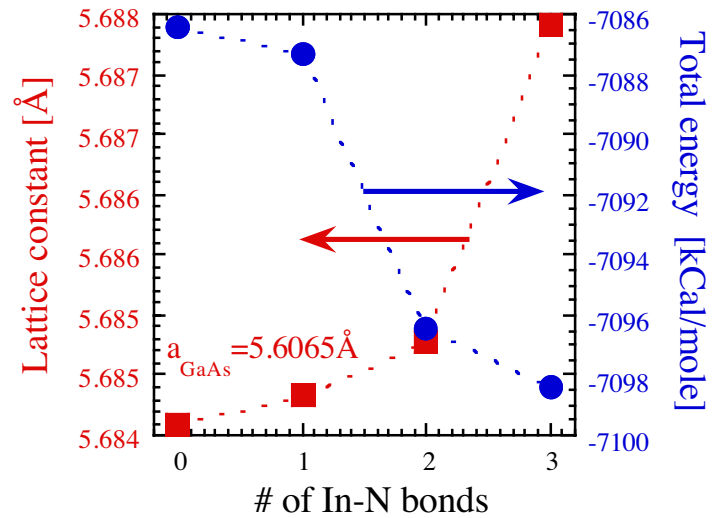
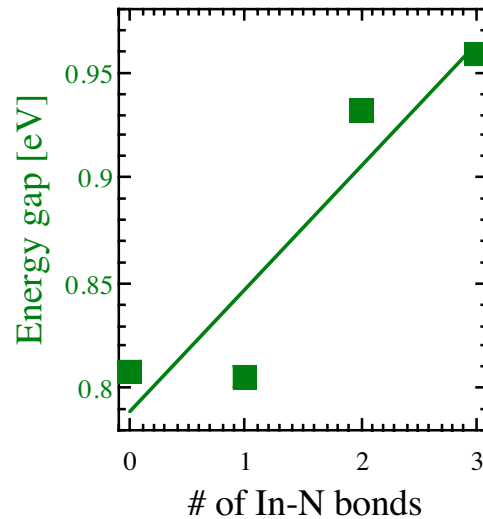
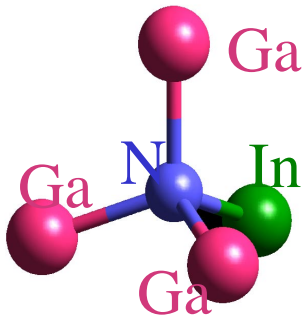
Telecommunications Application

- $\text{Ga}_x\text{In}_{1-x}\text{N}_y\text{As}_{1-y}$ ($x \approx 0.70$, $y \approx 0.03$) has a bandgap of $\sim 1.3 - 1.55 \mu\text{m}$
- It is nearly lattice-matched to GaAs
- Fabrication of inexpensive surface-emitting lasers for optoelectronics
- Optical fibers best at $\sim 1.3 - 1.55 \mu\text{m}$

Anneal GaInNAs to increase luminescence.

Problem: Band gap increases upon annealing

Nitrogen nearest neighbors affect optical properties



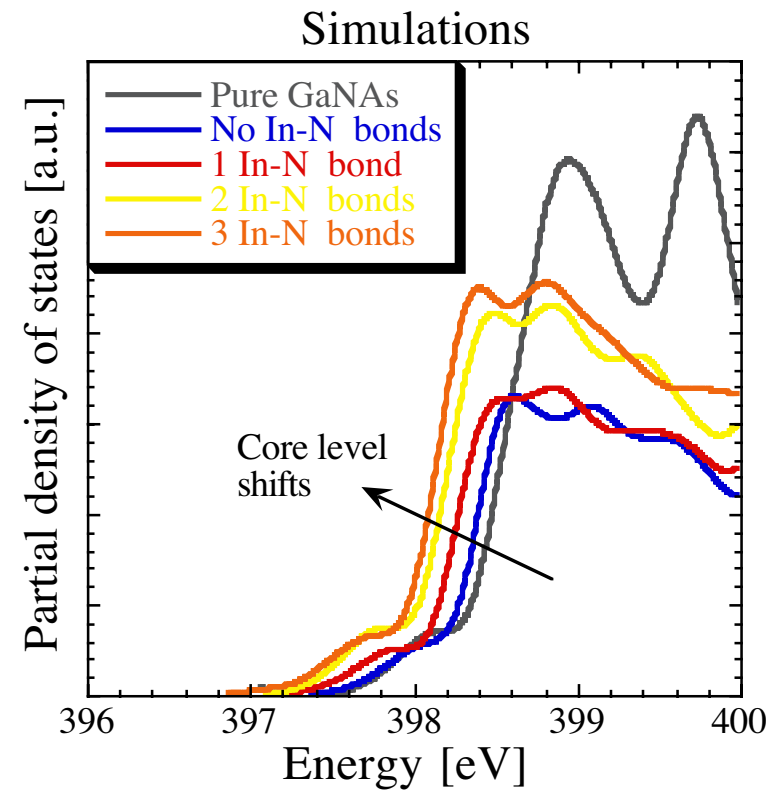
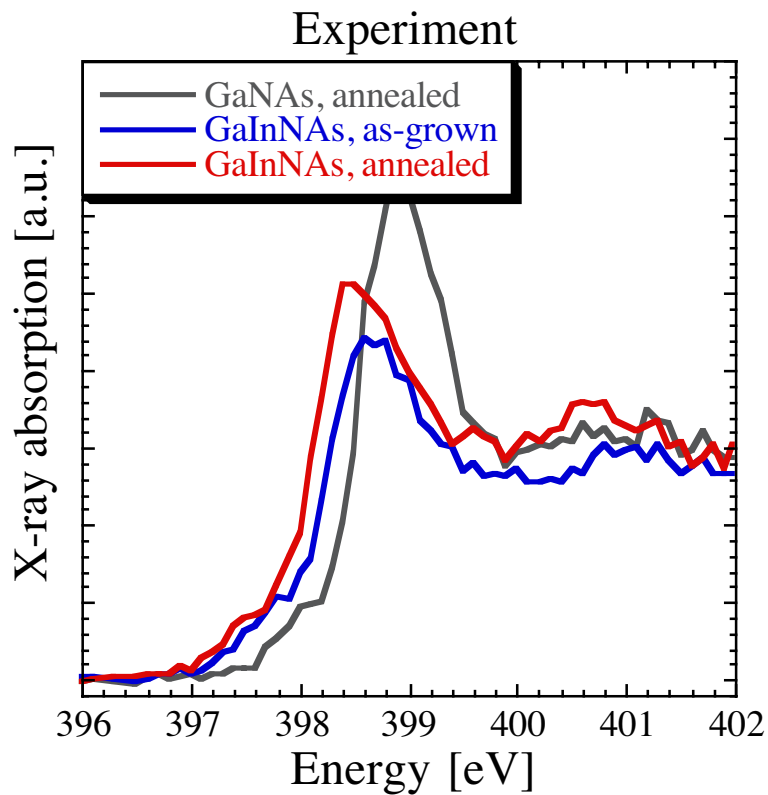
- MBE, ~2% nitrogen
- III-V random alloy
- FCC lattice

- Anneal at 780 °C, 1min
⇒ Luminescence increases
⇒ Bandgap increases

- Energy gap increases with # of In-N bonds

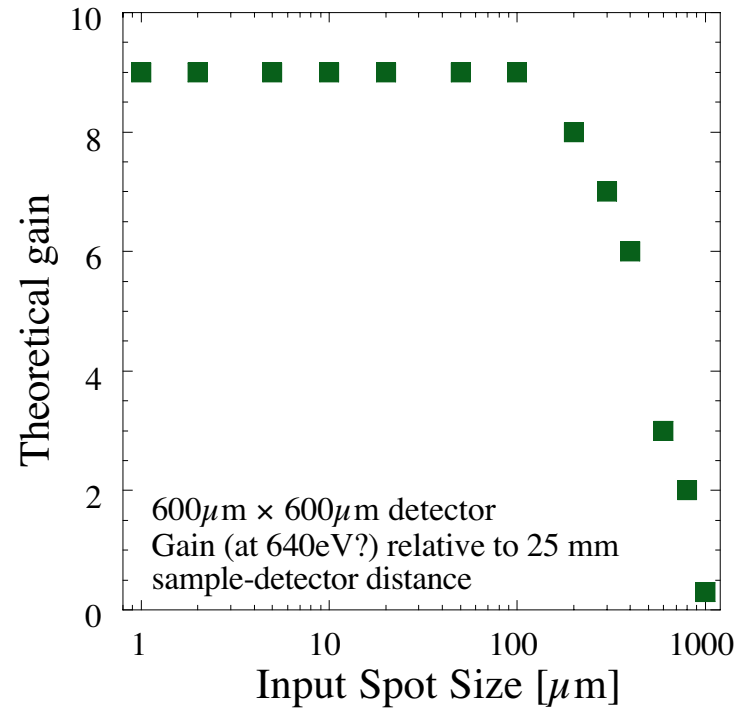
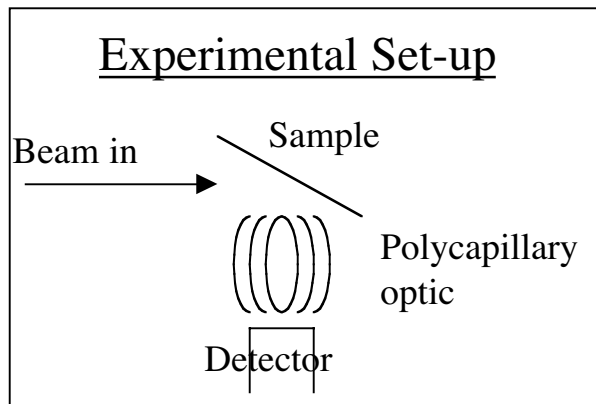
- Strain favors decreasing # of In-N bonds
- Thermodynamics favors increasing # of In-N bonds

Nitrogen X-ray absorption fine structure



Absorption edge shifts show increasing number of N-In bonds
Nitrogen migrates towards Indium upon annealing

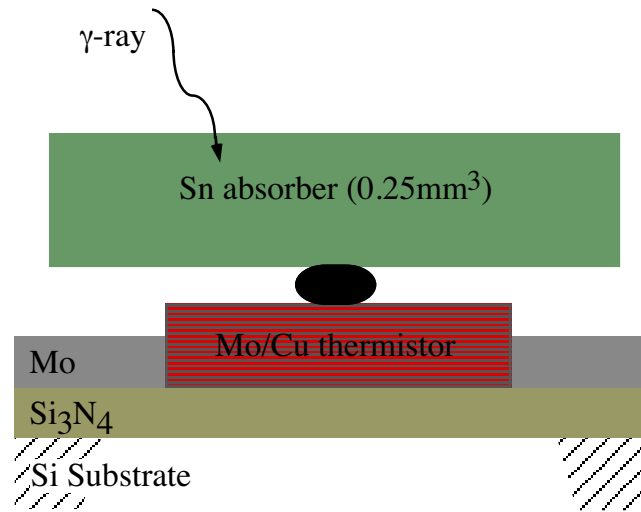
Current Work: Enhance Sensitivity



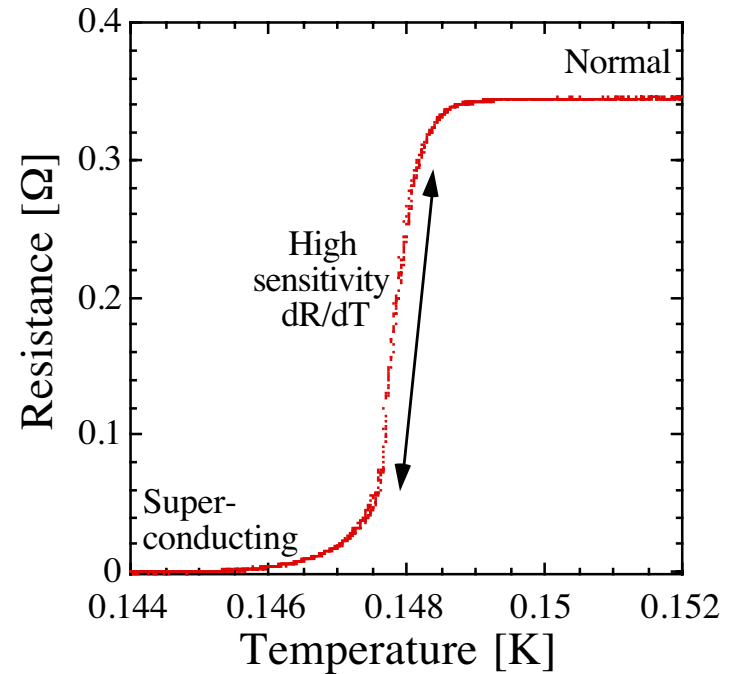
Spectrometer Development:

- Polycapillary Optic (courtesy XOS)
- Larger Arrays

Microcalorimeters



$$\text{Energy resolution } \Delta E_{\text{FWHM}} = 2.355 \sqrt{k_B T^2 C}$$



Ultra-high energy resolution thermal detectors require low operating temperature T and small volumes for low heat capacity C

Microcalorimeter Fabrication

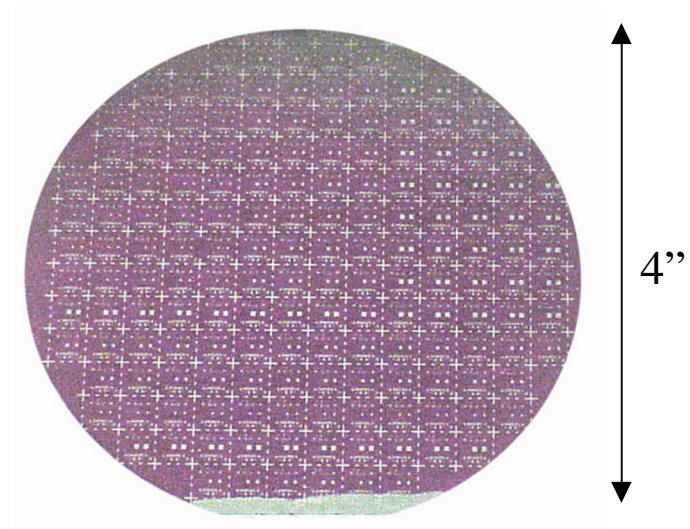
The Mo-Cu sensors are fabricated using photolithography like computer chips. Hundreds of identical devices are produced simultaneously on 4" wafers.

Mo/Cu thermal sensor:

- Fabricated at LLNL
- Stable, reproducible full-wafer process
- Flexible attached-absorber design

Application-specific absorbers:

- γ -rays: Sn crystal
- Neutrons: MgB_2 , LiF crystal (so far)
- X-rays: Au film

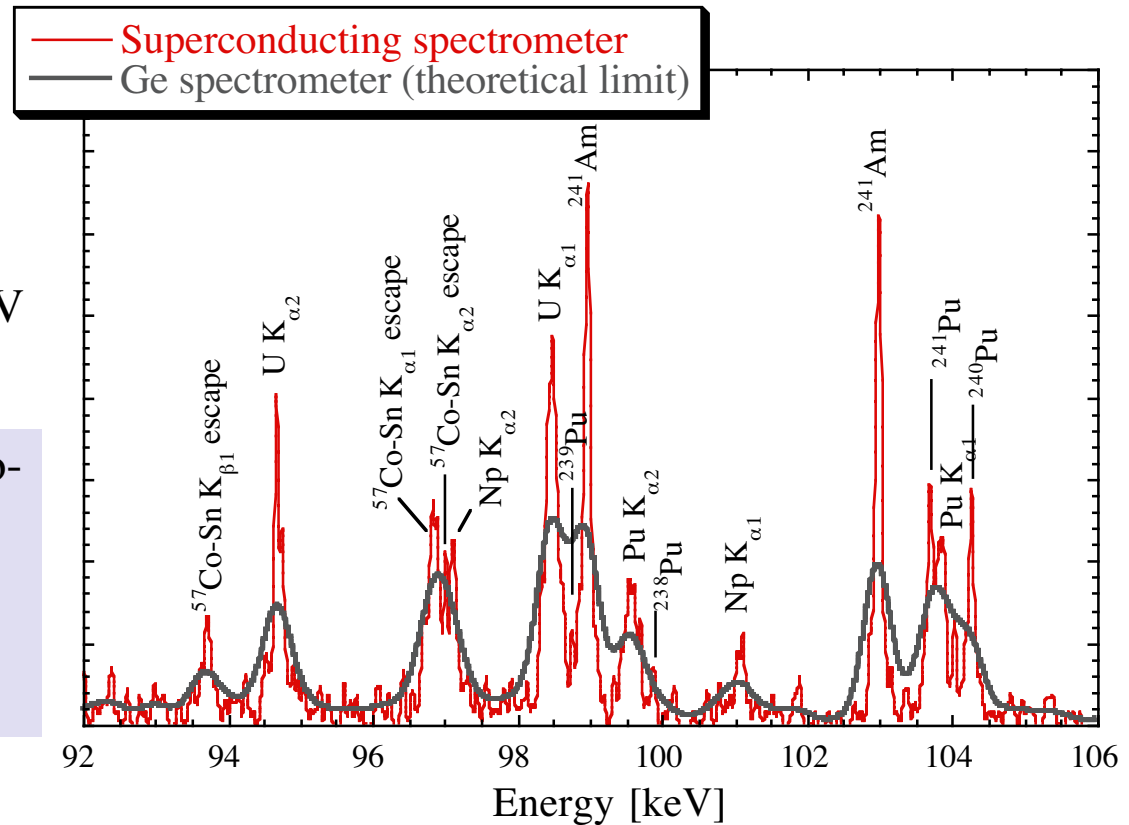


Gamma Ray Spectrometry

First measurements of SNM: Pu mixed isotope sample

$$\Delta E_{\text{FWHM}} \approx 60\text{-}90\text{eV at } 100\text{keV}$$

Superconducting γ -ray spectrometers enable high-resolution spectroscopy in cases where Ge detectors fundamentally limited by device physics.



Microcalorimeter Multiplexing

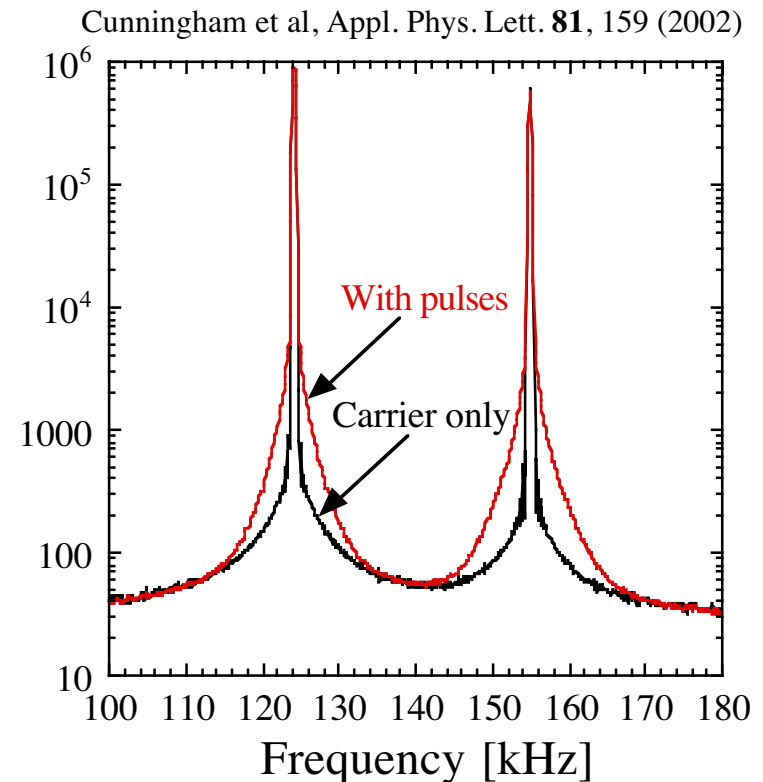
We can increase the area, count rate capabilities and sensitivity by frequency multiplexing many detector channels with a single SQUID preamplifier.

Present:

- dc and ac biased devices have same high resolving power $E/\Delta E \geq 1000$
- Single and multiplexed devices have same high resolving power $E/\Delta E \geq 1000$

Future:

- Single SQUID can multiplex ~ 30 sensors
- ~ 30 SQUIDs could offer three orders of magnitude improvement in sensitivity.

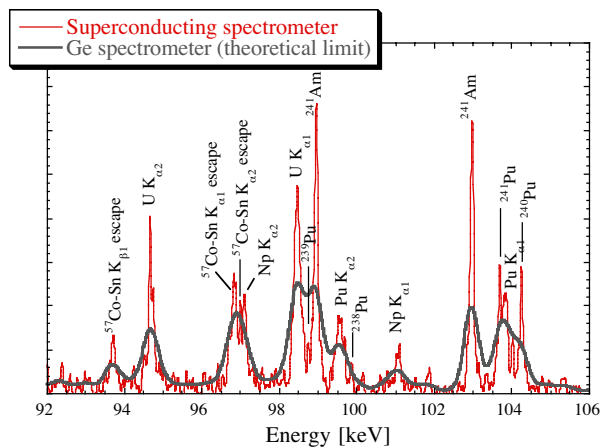


Summary

High-resolution cryogenic detector development

- Cryogenic spectrometer with cold finger
- 9-Channel STJ Arrays for synchrotron science
< 10-20 eV FWHM up to 1keV, > 100,000 counts/s
- Microcalorimeters for nuclear analysis
<100 eV FWHM for γ -rays below 100 keV

Frequency-multiplexing



X-ray and γ -ray Spectroscopy

- Increased In-N bonding explains widened bandgap in GaInNAs upon annealing
- First γ -ray measurements on special nuclear materials (multiplexed).